

# Impact of Superconductor LK-99 on Quantum Computers Maintenance and Operational Costs.



Adam S. Dahshan, Kareem Walid, STEM High School for Boys - 6<sup>th</sup> of October.

Research Supervisor: Ahmed S. Ahmed, STEM High School for Boys - 6<sup>th</sup> of October & Miami University Sophomore.

## Abstract

This research explores the impact of the superconductor LK-99 on the maintenance and operational costs of quantum computers. Quantum computers have shown great potential in revolutionizing computing by leveraging the principles of quantum mechanics to achieve exceptional computational power. However, the fragility of qubits - the fundamental units of quantum computing - poses significant challenges in terms of errors and decoherence. Efficiently managing quantum errors requires complex error correction techniques and the cooling of qubits to ultra-low temperatures. The concept of room-temperature superconductivity, exemplified by LK-99, offers a transformative solution by potentially reducing the cooling requirements of quantum hardware. This breakthrough could enhance the stability and viability of quantum devices for widespread utilization. This paper investigates the potential benefits of LK-99 in quantum computer operations, highlighting their role in mitigating thermal noise and improving qubit stability. The findings provide valuable insights into the practical implications of integrating superconductors in quantum computing systems, paving the way for more efficient and cost-effective utilization of these powerful machines.

## I. Introduction

Supercomputers have brought about a big change by effectively addressing complex scientific challenges that were previously obstacles for researchers. Their remarkable capacity to expediently execute Complicated algorithms, compressing the timeline of tasks from weeks to

minutes compared to classical computers, and their ability to simulate atomic-level behaviors of molecules have played fundamental roles in scientific advancements. Even with all the potential they hold, supercomputers have their limitations when compared to the enormous potential of quantum computers, which are still

in development but show great promise. The potential of quantum computers becomes conspicuously evident through their exceptional accomplishments. Google's Sycamore, a quantum computer boasting 53 qubits—the foundational units of quantum computing—successfully tackled the formidable BosonSampling problem within a mere 200 seconds. In stark contrast, conventional computers would require billions of years to achieve the same feat. Another noteworthy instance is the Fugaku quantum computer at the University of Tokyo, which adeptly emulated the intricate process of protein folding, a pivotal pursuit in drug development. Additionally, the University of Maryland employed quantum computers to replicate the behaviors of Ising model quantum magnets, thereby unveiling insights into quantum phenomena. These instances underscore the precision and intricacy of quantum simulations, underscoring the profound influence of quantum computing by yielding groundbreaking advancements. These quantum milestones are made possible by leveraging the tenets of quantum mechanics, particularly "superposition" and "quantum entanglement." Superposition engenders data parallelism, where quantum bits (qubits) exist in multiple states simultaneously, empowering quantum computers to navigate an extensive array of possibilities within a single computation. This capability significantly accelerates specific

problem-solving scenarios. Furthermore, the phenomenon of quantum entanglement permits interconnections among qubits, enabling the instantaneous influence of one qubit's state on another, even across significant distances. This property empowers quantum computers to execute intricate operations and simulations that surpass the capabilities of classical computers.

Quantum computers distinguish themselves from their supercomputer counterparts through various pivotal disparities. Foremost is the fundamental distinction in their data storage mechanisms. Supercomputers utilize "classical bits," while quantum computers use "qubits." This distinctive attribute empowers quantum computers to simultaneously explore an array of outcomes, thus setting them apart in computational efficacy. Furthermore, quantum computers leverage specialized tools known as "quantum gates," a departure from the conventional "logical gates" in supercomputers. These quantum gates facilitate the manipulation of qubits, enabling the execution of multifaceted algorithms, which address intricate challenges like factorization of large numbers or unsorted database searches.

As mentioned, quantum computing holds the promise of revolutionizing computations. Yet, this potential faces significant hurdles stemming from the fragility of qubits. Analogous to classical bits, qubits are vulnerable to

"decoherence," where their quantum states lose coherence due to environmental interactions. This leads to fidelity reduction and quantum computation errors, which amplify the risk of inaccuracies in quantum algorithms.

Environmental factors further compound qubit decoherence. Temperature fluctuations and electromagnetic radiation can destabilize the quantum states of qubits, accentuating the need to shield qubits from such interactions. Quantum errors encompass inaccuracies in quantum computations stemming from various sources, including qubit decoherence, gate imperfections, and readout inaccuracies. Addressing these errors necessitates intricate error correction techniques that leverage redundancy to enhance the stability of quantum computations.

Efficiently managing quantum errors involves cooling qubits to ultra-low temperatures, nearing absolute zero, to mitigate thermal noise and thus reduce qubit decoherence. Cryogenic systems and innovative cooling methods have emerged as critical tools for maintaining qubit stability and fidelity. Notably, the concept of room-temperature superconductivity offers a transformative avenue in quantum computing. Identifying materials that exhibit superconductivity at or near room temperature could substantially alleviate the cooling requirements of quantum hardware. This breakthrough could streamline quantum device

operations, making them more viable for widespread utilization. This paper will explore the distinction between classical bits and qubits, the fundamental units of information in supercomputers and quantum computers. It will also cover the three primary types of quantum computers—gate-based, Annealing-Based, and superconducting quantum computers—alongside the cooling process, popular superconductors, and implementations of LK-99.

## **II. Quantum Bits**

Within the world of computing, the conventional method of storing information relies on classical bits—fundamental units characterized by two states: 0 (off) or 1 (on). These binary representations are subsequently translated into data embedded within the web of a computer system. However, this conventional approach carries inherent limitations. Notably, it necessitates longer processing times for intricate simulations and the resolution of complex equations. These time-intensive endeavors arise due to the nature of classical bits, which can occupy only one state at a given moment. Nevertheless, this limitation doesn't imply a barrier to computational advancements. [1]

In recent developments, quantum computers have emerged as a promising avenue for overcoming these challenges. While still in their early stages of development, quantum computers aim to address the shortcomings of current

classical systems. A significant step in this direction involves reimagining the fundamental unit of information—moving from classical bits to qubits. Qubits distinguish themselves from bits across multiple parameters, with one noteworthy distinction being their reliance on principles derived from quantum mechanics. Notably, qubits harness the concepts of "superposition"

$$|\psi\rangle = a|0\rangle + b|1\rangle$$

Figure 1: Qubit wave equation.

and "quantum entanglement" to their advantage. Qubits can exist at multiple states at the same time where its state will be shown in the wave equation  $|\psi\rangle = \alpha|0\rangle + \beta|1\rangle$ , where  $\alpha$  and  $\beta$  are complex numbers that determine the probability amplitudes of the qubit being in states 0 and 1 respectively. [2]

This ability, influenced by quantum gates, enables the computer to process multiple cases simultaneously.

A key quantum gate in this context is the Hadamard Gate (H), which facilitates the creation of a superposition state denoted by  $H = \frac{1}{\sqrt{2}} \begin{bmatrix} 1 & 1 \\ 1 & -1 \end{bmatrix}$ . Additionally, the pauli gates—pauli-X, pauli-Y, and pauli-Z—play vital roles in phase change and qubit manipulation. These gates are represented by  $X = \begin{bmatrix} 0 & 1 \\ 1 & 0 \end{bmatrix}$ ,  $Y = \begin{bmatrix} 0 & -i \\ i & 0 \end{bmatrix}$ ,  $Z = \begin{bmatrix} 1 & 0 \\ 0 & 1 \end{bmatrix}$  respectively. [3]

$$\begin{array}{c} \boxed{X} \quad \boxed{Y} \quad \boxed{Z} \quad \boxed{H} \\ \left( \begin{array}{cc} 0 & 1 \\ 1 & 0 \end{array} \right) \quad \left( \begin{array}{cc} 0 & -i \\ i & 0 \end{array} \right) \quad \left( \begin{array}{cc} 1 & 0 \\ 0 & -1 \end{array} \right) \quad \frac{1}{\sqrt{2}} \left( \begin{array}{cc} 1 & 1 \\ 1 & -1 \end{array} \right) \end{array}$$

Figure 2: Pauli-X, Y, Z and Hadamard gates [70]

Another significant concept underlying the quantum system is Schrödinger's equation, which measures changes in a function over time. It's represented as  $i\hbar \frac{d}{dt} |\psi(t)\rangle = H|\psi(t)\rangle$ . A notable algorithm that capitalizes on the concept of superposition is Grover's algorithm for searching unsorted lists. It employs multiple Hadamard gates to bring the qubit into an even superposition state. Further, Pauli-Z gates amplify the wave function's amplitudes to move closer to the desired answer, achieved through a process called the Oracle. [4]

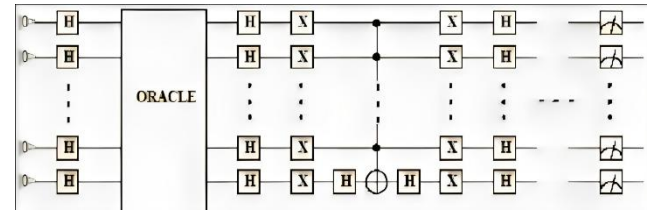


Figure 3: An inside depiction of the Grover's algorithm [71]

Quantum entanglement, a captivating aspect of qubits, allows them to establish an intangible connection—resembling an imaginary string—regardless of the physical distance between them. This entanglement profoundly influences the states of the connected qubits, opening new vistas to transcend classical computing. Quantum teleportation exemplifies this phenomenon by

transmitting the state of one qubit from a source to a distant location. This concept holds potential applications in distributed quantum computing, enabling the efficient transfer of qubit states to different processors for enhanced problem-solving capabilities. The process of quantum teleportation involves manipulating an entangled pair of qubits, with one serving as the sender qubit and the other as an additional qubit. [5, 6]

In essence, operations are executed on the sender qubit, along with the qubit intended for teleportation and the additional qubit. These

$$\begin{aligned} |\Phi^+\rangle &= \frac{|00\rangle + |11\rangle}{\sqrt{2}} & |\Psi^+\rangle &= \frac{|01\rangle + |10\rangle}{\sqrt{2}} \\ |\Phi^-\rangle &= \frac{|00\rangle - |11\rangle}{\sqrt{2}} & |\Psi^-\rangle &= \frac{|01\rangle - |10\rangle}{\sqrt{2}} \end{aligned}$$

Figure 4: The 4 bell states.

operations, represented as classical bits, are transmitted to the receiving end, where specific actions are taken to transform the receiving qubit's state into the desired state. These actions correspond to what is known as bell operations or bell states. These states are encapsulated in four equations—Phi Plus ( $|\Phi^+\rangle$ ), Phi Minus ( $|\Phi^-\rangle$ ), Psi Plus ( $|\Psi^+\rangle$ ), and Psi Minus ( $|\Psi^-\rangle$ ). Each equation describes the entanglement nature between two qubits. For instance,  $|\Phi^+\rangle = \frac{1}{\sqrt{2}} (|00\rangle + |11\rangle)$ ,  $|\Phi^-\rangle = \frac{1}{\sqrt{2}} (|00\rangle - |11\rangle)$ ,  $|\Psi^+\rangle = \frac{1}{\sqrt{2}} (|01\rangle + |10\rangle)$ , and  $|\Psi^-\rangle = \frac{1}{\sqrt{2}} (|01\rangle - |10\rangle)$ . These states also offer insights into the relationships

between entangled qubits and find utility in quantum error correction and addressing the challenges posed by decoherence. [7]

The distinction between classical and quantum computers extends beyond their methods of data representation; it encompasses the very process of extracting information from operations. In classical computing, data retrieval involves a precision-oriented approach, where data is extracted with exact accuracy by sequentially reading the bit sequence stored in the computer's memory. Quantum computers, however, adopt a fundamentally different strategy for extracting data. Instead of yielding a single definitive result, quantum operations generate a spectrum of potential outcomes. Through repeated execution of these operations, varied results emerge in each instance. Subsequently, these outcomes are compiled, and a statistical analysis is employed to derive insights regarding the probabilities associated with each feasible outcome.

The probabilistic nature inherent in data acquisition using qubits introduces a critical concern involving two phenomena: decoherence and quantum noise. These factors exert adverse influences on the accuracy of qubit data. Decoherence and quantum noise arise due to shared reasons, primarily linked to external environmental interactions. Ultraviolet radiation emitted by the sun and temperature fluctuations during the computer's operational runtime serve

as primary triggers for these phenomena. Consequently, an array of types of quantum computing is devoted to mitigating the impact of decoherence and quantum noise. [8-10]

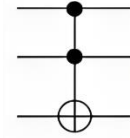
### III. Types of Quantum Computers

#### *Gate-based quantum computers*

Gate-based quantum computing, a cornerstone of quantum computational paradigms, relies on the orchestration of quantum gates as its foundational building blocks. These gates wield the power to manipulate the quantum states of qubits and pave the way for the execution of intricate quantum algorithms. Quantum gates are often represented by unitary matrices (U) and serve as the linchpin for quantum computation, playing a pivotal role in the processing of quantum information.

An inherent property of quantum gates is their ability to create entanglement between qubits. When two or more qubits are entangled, the state of one qubit  $|\psi\rangle$  is inherently dependent on the state of another, even when physically separated. This phenomenon of entanglement constitutes a bedrock for various quantum algorithms and quantum error correction schemes [11, 12].

One quantum gate of remarkable significance is the Toffoli gate, colloquially known as the Controlled-Controlled-Not (CCNOT) gate.



$$\text{CCNOT} = \begin{pmatrix} 1 & 0 & 0 & 0 & 0 & 0 & 0 & 0 \\ 0 & 1 & 0 & 0 & 0 & 0 & 0 & 0 \\ 0 & 0 & 1 & 0 & 0 & 0 & 0 & 0 \\ 0 & 0 & 0 & 1 & 0 & 0 & 0 & 0 \\ 0 & 0 & 0 & 0 & 1 & 0 & 0 & 0 \\ 0 & 0 & 0 & 0 & 0 & 1 & 0 & 0 \\ 0 & 0 & 0 & 0 & 0 & 0 & 0 & 1 \\ 0 & 0 & 0 & 0 & 0 & 0 & 1 & 0 \end{pmatrix}$$

Figure 5: CCNOT gate matrix.

This three-qubit quantum gate enacts a controlled-controlled-X (CCX) operation on its target qubit. In classical computing parlance, it resembles a logical AND gate controlled by two input bits— $|a\rangle |b\rangle$ —and employed to toggle the state of a target bit— $|c\rangle$ . The Toffoli gate is represented by the equation:  $|a\rangle |b\rangle |c\rangle \rightarrow |a\rangle |b\rangle |c \oplus (a \wedge b)\rangle$  where  $|a\rangle$ ,  $|b\rangle$ , and  $|c\rangle$  represent the states of the three qubits and " $\oplus$ " denotes the bitwise XOR operation, which means that the state of the target qubit  $|c\rangle$  is flipped (X gate applied) if and only if both control qubits  $|a\rangle$  and  $|b\rangle$  are in the state  $|1\rangle$ . This gate finds itself ubiquitously integrated into quantum circuit design, playing an indispensable role in the orchestration of quantum algorithms and quantum error correction procedures [13-16].

Quantum error correction mechanisms emerge as an imperative facet in gate-based quantum computers, addressing the intrinsic susceptibility of qubits to errors stemming from multifarious sources. These errors include qubit decoherence ( $\Gamma$ ), environmental interactions, and quantum noise. Quantum error-correcting codes (QECCs) occupy a pivotal position in this context,

bolstering the reliability of quantum computations. QECCs introduce redundancy by encoding logical qubits across multiple physical qubits, obviating the need for direct measurements. Error detection syndromes are meticulously assessed to pinpoint errors, and corrective operations are judiciously applied to restore the encoded quantum state [17-19].

The SWAP gate, a fundamental two-qubit quantum gate, assumes a prominent role in quantum computing. Its core function lies in the exchange of quantum states between two qubits. Analogous to its classical counterpart that swaps the values of classical bits. The representation of the SWAP gate is  $|a\rangle|b\rangle \rightarrow |b\rangle|a\rangle$  and even if the first qubit  $|a\rangle$  is in a superposition or any quantum state, the SWAP gate effectively swaps its state with the second qubit  $|b\rangle$ . This operation underpins multi-qubit operations, facilitating the implementation of intricate quantum algorithms [20].

Gate-based quantum computers engage in a symphony of individual qubit operations, encompassing rotations and flips. These elementary operations, often represented as quantum gates (U), collectively contribute to the realization of complex quantum algorithms, allowing quantum computations to unfold in a meticulously choreographed manner.

Quantum circuits, serving as visual blueprints of quantum algorithms, assume a pivotal role in

quantum computing. These circuits are an amalgamation of quantum gates and operations, meticulously sequenced to delineate the step-by-step computational journey. The Quantum Fourier Transform (QFT), often represented by a unitary operator (U), stands as a quintessential example, facilitating a quantum rendition of the discrete Fourier transform—a critical operation in the quantum domain. QFT transmutes an input quantum state  $|a\rangle$  into another quantum state  $|b\rangle$  nestled within the frequency or Fourier basis.

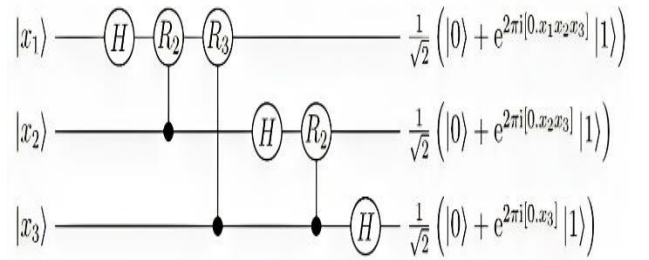


Figure 6: Depiction of the QFT's process of state exchange

This transformative feat finds application in a spectrum of quantum algorithms, including Shor's algorithm for integer factorization and quantum phase estimation [21-25].

The Quantum Phase Estimation (QPE) algorithm, a cornerstone of quantum computing, emerges as a potent tool for the estimation of phase ( $\phi$ ) or eigenvalues of a unitary operator.

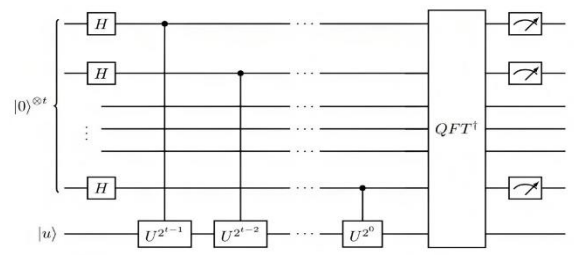


Figure 7: Depiction of the Quantum Phase Estimation Algorithm (QPE)



QPE's importance reverberates through various quantum algorithms, including the trailblazing Shor's algorithm and quantum simulations. This algorithm plays a pivotal role in deciphering intricate problems in cryptography and quantum system simulations [26-28].

In the realm of quantum computing, where combinatorial optimization problems pose formidable challenges, the Quantum Approximate Optimization Algorithm (QAOA) emerges as a beacon of hope. QAOA is a hybrid quantum-classical algorithm meticulously designed to tackle such conundrums. It embarks on its quest by translating the problem's solution space into a quantum state. QAOA operates through a sequence of quantum circuit layers, each composed of a quantum mixer unitary  $U_m$  for entanglement creation and a problem-specific cost unitary  $U_c$  encoding the objective function. Following a variational approach, the algorithm optimizes the circuit's parameters to approximate the optimal solution. At each iteration, measurements are meticulously taken to evaluate the objective function, with classical optimization techniques fine-tuning circuit parameters. QAOA continues this iterative process until a predefined convergence criterion is met, striving to unearth a quantum state that faithfully approximates the optimal solution to the intricate optimization problem. This endeavor holds the promise of delivering a quantum speedup across a myriad of

applications, thus underlining the transformative potential of quantum computing [29, 30].

### *Annealing-based quantum computers*

Annealing-based quantum computers, also known as quantum annealers, represent a distinct category of quantum computing devices meticulously engineered for the resolution of optimization problems. These cutting-edge devices find their forefront in the work of D-Wave Systems, a leading entity in quantum computing technology.

The underlying operational principle of annealing-based quantum computers revolves around a process known as quantum annealing. This technique harnesses the inherent inclination of quantum systems to converge towards low-energy states, rendering it invaluable in the domain of optimization problems. Quantum annealing offers a novel approach compared to classical annealing, which explores energy landscapes iteratively. Instead, quantum annealing taps into quantum tunneling and fluctuations, enabling the agile navigation of a more extensive solution space.

In the realm of annealing-based quantum computers, problems are aptly translated into discrete energy levels. The ultimate objective is to discern the configuration characterized by the lowest energy state, signifying the optimal solution. Hence, annealing-based quantum



computers commence by initializing qubits in a superposition of states, facilitating the simultaneous exploration of multiple potential solutions. This fundamental concept underpins the efficient traversal of solution spaces [31].

The Ising model emerges in the form of a powerful mathematical tool, acting as a faithful representation of interacting spins within a given system. It forms the linchpin for various optimization-related issues. Annealing-based quantum computers ingeniously map these intricate optimization problems onto Ising Hamiltonians, thus transforming real-world conundrums into energy-minimization tasks tailor-made for quantum computation [32].

Crucially, quantum tunneling emerges as a formidable ally, empowering qubits to surmount energy barriers. This capability enables them to explore the profound solution valleys nestled within the problem's vast landscape. Quantum fluctuations enter the equation, introducing an element of probabilistic behavior. This facet allows annealing-based quantum computers to traverse a rich tapestry of states, ultimately culminating in the pinpointing of optimal solutions. The advent of annealing-based quantum computers heralds a transformative era in the domain of optimization problems, offering new vistas for tackling complex real-world challenges [33, 34].

## ***Superconducting Quantum Computers***

New territory within quantum computing is being explored through superconducting quantum computers, currently in the stages of development. This emerging approach aims to tackle the persistent challenge of decoherence, which affects other types of quantum computers due to interactions with their environment, including gamma rays and temperature fluctuations. A key issue arises as qubits move through circuits, creating heat through friction and resistance. This thermal effect leads to quantum noise, disrupting the integrity of quantum information in the qubits and causing inaccuracies in measurements.

Superconducting quantum computers introduce an innovative solution by using a specific type of qubit called superconducting qubits. This approach integrates the unique properties of superconducting materials with the principles of qubits. The result is qubits with extremely low resistance and high conductivity, effectively minimizing heat generation, reducing quantum noise, and countering the negative impacts of decoherence.

A distinctive part of superconducting quantum computers that sets them apart from other quantum computer types is the Josephson junction. This integral element plays a crucial role in establishing the necessary energy level structure for various aspects of qubit

manipulation and coherent control over quantum states, as well as facilitating the creation process of superconducting qubits. The Josephson junction primarily consists of two superconducting electrodes, separated by a thin oxide insulating barrier that enables the flow of supercurrent across the junction. [38, 39]

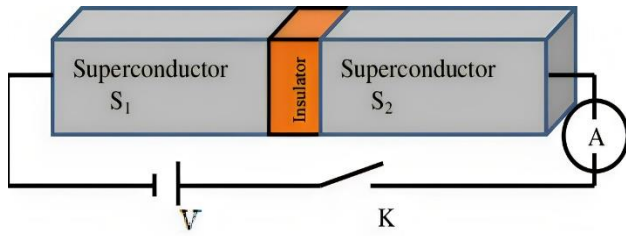


Figure 8: A figure illustrating the Josephson Junction [72]

The pivotal function of the Josephson junction lies in its ability to introduce nonlinearity into the superconducting circuit, a property essential for controlling energy levels. This nonlinearity arises from the sinusoidal current-phase relationship described by the Josephson equation:  $I = I_c \sin(\delta)$ . Here,  $I$  signifies the supercurrent coursing through the Josephson junction—a current flowing without resistance in a superconducting material.  $I_c$  denotes the critical current of the Josephson junction, representing the maximum current that can flow through the junction while maintaining its superconducting state.  $\delta$ , which can be expressed as  $e^{i\delta}$ , encapsulates the phase difference across the Josephson junction. This phase difference corresponds to the variance in angles between the quantum mechanical wave functions on either

side of the Josephson junction. By accurately adjusting this current, the energy levels within the system can be precisely controlled. This manipulation of energy levels empowers the execution of qubit operations, enabling the superconducting quantum computer to perform complex computations that wouldn't be feasible using classical computers. [38, 39]

Superconducting qubits encompass three primary types: the flux qubit, Transmon qubit, and xmon qubit.

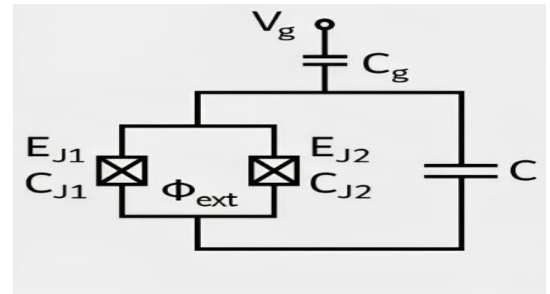


Figure 9: Illustration of the manipulation circuit of the Transmon qubit [74]

The flux qubit features a configuration comprising a superconducting loop that contains one or more interruptions via Josephson junctions. The behavior of this qubit is intricately tied to the loop's geometry and the number of Josephson junctions present.

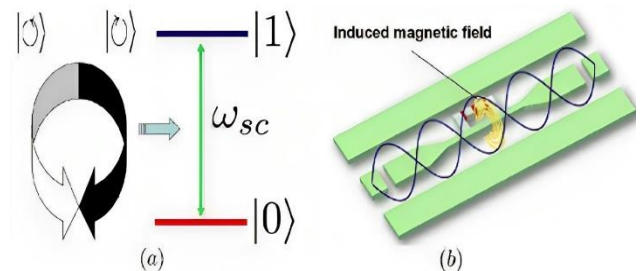


Figure 10: An illustration of the superconducting loop of the Flux qubit.

Crucially, the flux qubit's states are determined by the magnetic flux that traverses the loop, a factor controllable through external magnetic fields. [35, 36, 41]

The energy characteristics of the flux qubit are mathematically encapsulated within the Hamiltonian equation:  $H = \frac{\hbar}{2}(E_m\sigma_z - E_J\cos(\phi)\sigma_x)$ . wherein,  $H$  represents the Hamiltonian operator governing the qubit's energy states.  $\hbar$  denotes the reduced Planck constant, where  $\hbar = \frac{h}{2\pi}$ .  $E_m$  signifies the energy difference between the two lowest energy states of the qubit, while  $E_J$  pertains to the Josephson energy—the parameter dictating the behavior of the Josephson junction.  $\phi$  is the magnetic flux in the junction's loop.  $\sigma_z$  and  $\sigma_x$  are the pauli-Z and pauli-X matrices. [36, 37, 38, 39, 41]

Flux qubits offer distinct advantages, including strong anharmonicity, which renders them less susceptible to specific types of noise in contrast to other qubit variants. This attribute contributes to their resilience in certain noise-laden environments. However, it's important to note that flux qubits can exhibit sensitivity to fluctuations in magnetic fields, underscoring the need for meticulous control and shielding measures to ensure accurate quantum operations. [35, 36, 41]

Among the superconducting qubit variants, the transmon qubit emerges as a significant

contender. Its architecture entails a superconducting island—comprising a small piece of superconducting material—interconnected with a ground plane through Josephson junctions. A shunting capacitor runs in parallel with these junctions, effectively reducing the qubit's charging energy. This reduction results in nearly equidistant energy level spacings, a condition known as the "transmon regime." This regime amplifies the qubit's coherence attributes, as equidistant energy levels thwart "spectral leakage," thereby enhancing resilience against specific noise sources. [35, 36, 41]

The transmon qubits can be manipulated using microwave signals, and it is measured out through microwave resonators that are coupled to the qubit. While the equidistant energy levels significantly bolster coherence duration and noise resistance, a tradeoff surfaces. [35, 36, 41]

The proximate arrangement of energy levels, although advantageous for these characteristics, can complicate specific quantum operations and gate manipulations. This relationship could potentially introduce challenges to the precision of execution, thereby influencing the overall fidelity of quantum computations.

An extensively favored design within the realm of superconducting qubits is the xmon qubit, renowned for its adaptability and seamless integration with diverse circuits. Xmon qubits

share the foundational characteristics of transmon qubits, augmented by a distinctive cross-shaped geometry that imparts heightened coherence attributes and improved coupling to microwave resonators.

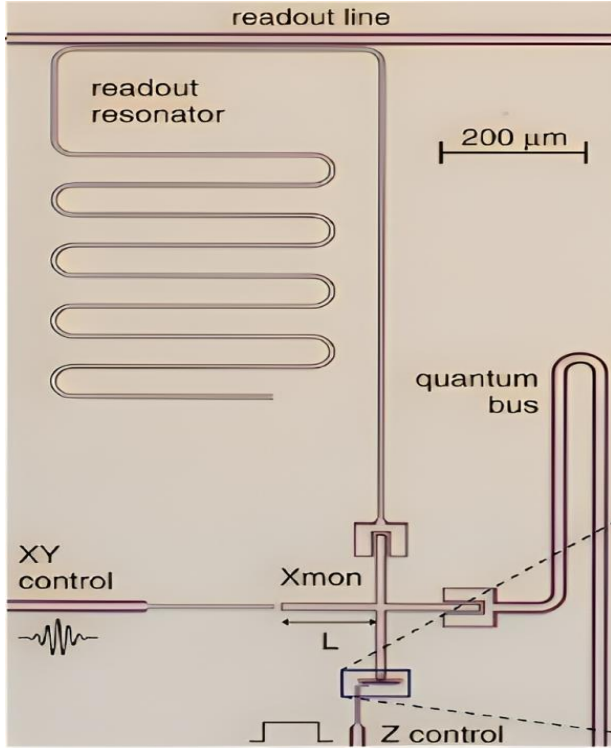


Figure 11: Illustration of the circuit for Xmon qubit manipulation [75]

Notably, xmon qubits possess a pivotal advantage that has propelled their widespread adoption: compatibility with circuit QED (Quantum Electrodynamics) configurations, which rank among the most prevalent circuit architectures employed in the domain of superconducting quantum computing. [40-42]

Quantum Electrodynamics (QED) circuits constitute a foundational framework that endeavors to integrate quantum mechanical

principles with the functionality of qubits and resonators. These intricate circuits encompass two primary components: superconducting qubits, predominantly in the form of Transmon or Xmon qubits, and Microwave Resonators, which serve as electromagnetic cavities capable of trapping and confining microwave photons. [43, 44]

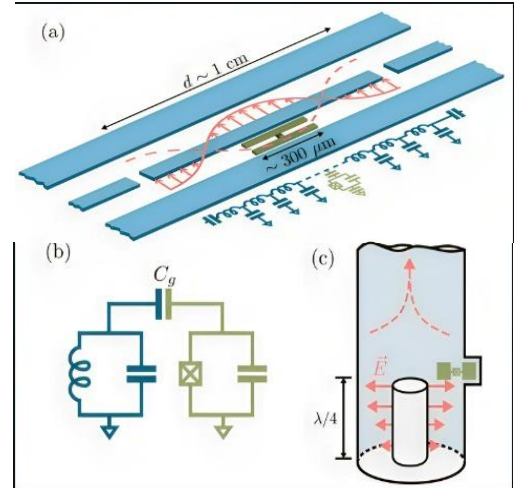


Figure 12 & 13: (a), (b), and (c) are different illustrations of the Quantum Electrodynamics circuit [76]

The essence of QED circuits lies in enabling the exchange of quantum information between qubits and resonators through the emission or absorption of microwave photons. This dynamic interaction is controlled by the presence of Josephson junctions within the qubits, allowing for the manipulation, creation, and annihilation of photons.

The interaction between qubits and microwave resonators finds mathematical expression through the Jaynes-Cummings model, which delineates the interplay between these elements.

The Hamiltonian governing this relationship is encapsulated as follows:  $H = \hbar\omega_r a^\dagger a + \frac{1}{2}\hbar\omega_q \sigma_z + \hbar g(a\sigma_+ + a^\dagger\sigma_-)$ . Here,  $\omega_r$  signifies the resonator frequency, symbolizing the energy associated with confined microwave photons. Operators  $a$  and  $a^\dagger$  denote the annihilation and creation operators for the resonator mode, respectively. The qubit frequency  $\omega_q$  reflects the energy spacing between the qubit's discrete energy levels, while  $\sigma_z$  represents the pauli-Z matrix. The qubit-resonator coupling strength is denoted by  $g$ .  $\sigma_+$  and  $\sigma_-$  signify the qubit's raising and lowering operators.

The efficacy of QED circuits extends to qubit readout, often accomplished through techniques like "dispersive readout setup." This method involves detuning the qubit and resonator from each other, generating an energy shift within the resonator frequency contingent on the qubit's state. By finely tuning this detuning, qubit measurements can be executed without disturbing their superposition state. This non-destructive approach enhances qubit coherence and permits multiple measurements to be gathered without compromising the qubit's integrity. The underlying frequency shift is approximated by the equation:  $\chi = \frac{g^2}{\Delta}$ , where  $\chi$  represents the frequency shift employed for qubit state measurements,  $g$  signifies the qubit-resonator coupling strength, and  $\Delta$  signifies the

detuning disparity between the qubit and resonator frequencies. [43, 44]

## IV. Cooling Process of QC

An indispensable pillar of quantum computing's success lies in the process of cooling, an essential process that reduces thermal noise, preserving the intricate quantum states indispensable for precise computation. At the core of quantum computing setups stands dilution refrigeration, a cooling method hinging on the properties of isotopes, mainly helium-3 and helium-4.

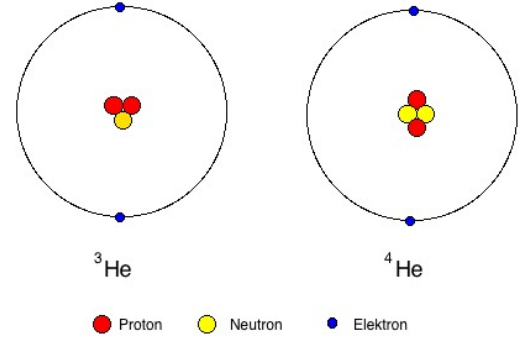


Figure 14: Atomic structure of  $\text{He}^3$  and  $\text{He}^4$

Through the mixing of the He isotopes, remarkable transformations transpire—a transition to a superfluid state. This transition results in a dramatic reduction in temperature [45].

Two fundamental principles, quantum degeneracy and the heat capacity of helium isotopes stand as the cornerstones dictating the dynamics of dilution refrigeration. Together, they facilitate the achievement of ultracold temperatures. The cooling process is a multistage endeavor, systematically extracting thermal

energy to craft a stable environment for qubits, thereby ensuring their unwavering stability and coherence.

One of the key principles governing the behavior of helium isotopes in this cooling process is described by the Debye Model expressed in this equation:

$$C_V = 9N\kappa\left(\frac{T}{\Theta_D}\right)^3 \int_0^{\frac{\Theta_D}{T}} \frac{x^4 e^x}{(e^x - 1)^2} dx$$
 . Where  $C_V$  represents the heat capacity,  $T$  is the absolute temperature, and  $\Theta_D$  is the Debye temperature, which characterizes the crystal lattice vibrations in the solid,  $N$  represents the total number of oscillators, and  $\kappa$  represents the Boltzmann constant, which is approximately  $1.38 \times 10^{-23}$ .

Adiabatic demagnetization refrigeration (ADR), an alternate cooling approach deployed in quantum computing, operates at the intersection of magnetic entropy and temperature dynamics.

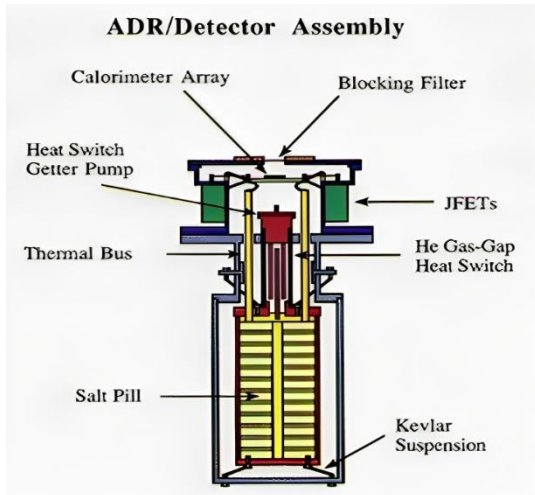


Figure 15: Illustration of an Adiabatic demagnetization refrigeration (ADR)

This process relies on the Adiabatic Demagnetization Equation:  $\Delta T = \frac{\mu_0 M}{C} \Delta B$  . Where  $\Delta T$  represents the change in temperature,  $\mu_0$  is the magnetic constant (permeability of free space),  $M$  is the magnetization of the material—The ratio of magnetic moment to the volume of the material—,  $C$  is the heat capacity of the material,  $\Delta B$  represents the change in magnetic field. The meticulous orchestration of magnetization and demagnetization cycles, as dictated by this equation, culminates in a marked reduction in temperature, crucial for quantum computing [46].

Pulse tube refrigeration ushers in an innovative era of quantum cooling methodologies. This approach relies on cyclic compression and gas expansion, facilitating heat extraction from the refrigeration stage. This heat is subsequently transported to the cold head, initiating the cooling process.

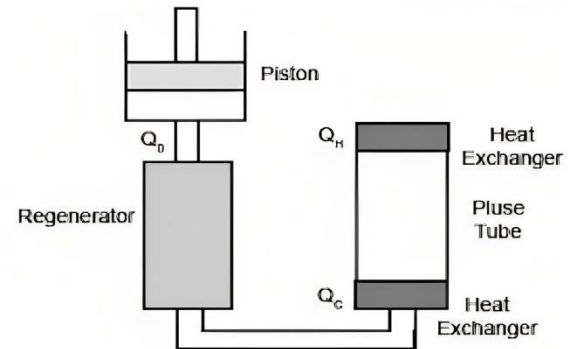


Figure 16: Illustration of the Pulse tube refrigeration [77]

In the realm of pulse tube refrigeration, the concept of Carnot Efficiency comes into play.

The Carnot Efficiency equation is a fundamental expression in thermodynamics, and it provides an upper limit on the efficiency of any heat engine or refrigerator. For a heat engine, the Carnot Efficiency ( $\eta_c$ ) is given by:  $\eta_c = 1 - \frac{T_C}{T_H}$ . Where  $T_C$  is the absolute temperature of the cold reservoir and  $T_H$  is the absolute temperature of the hot reservoir. Efficiency is a critical factor in pulse tube refrigeration, as it determines how effectively heat can be extracted from the system to achieve the desired cooling effect [47-49].

Helium, particularly isotopes  $\text{He}^3$  and  $\text{He}^4$ , plays a pivotal role in the cooling process of quantum computers. A significant distinction between these isotopes lies in their fermionic and bosonic nature.  $\text{He}^3$ , with one proton and two neutrons, possesses an odd number of fermions, classifying it as a fermion material. This distinction arises from the concept of fermions and bosons, each characterized by unique properties. Fermions exhibit half-integer quantum spin numbers ( $\pm \frac{1}{2}, \pm \frac{3}{2}$ ) stemming from their odd number of fermions. Conversely, bosons have even numbers of fermions, resulting in integer quantum spin numbers (-1, 0, 1) [50].

fermions' half-integer quantum spin numbers endow them with distinctive characteristics, notably the Pauli exclusion principle and Cooper pairing. The Pauli exclusion principle dictates that no two electrons within a system can occupy the same quantum state. Mathematically

represented as:  $\Psi(r_1, r_2, \dots, r_N, \sigma_1, \sigma_2, \dots, \sigma_N) = -\Psi(r_2, r_1, \dots, r_N, \sigma_2, \sigma_1, \dots, \sigma_N)$ , where  $\Psi$  represents the quantum wave function of the N-fermion system,  $r_i$  represents the spatial coordinates of the  $i$ -th fermion,  $\sigma_i$  represents the spin state of the  $i$ -th fermion, and The minus sign on the right side of the equation indicates that the wave function is antisymmetric with respect to the exchange of two fermions.

Cooper pairing, another unique property of fermions facilitated indirectly by the Pauli exclusion principle, is a quantum mechanical phenomenon observed when fermions interact through attractive forces, often due to lattice vibrations called phonons. Cooper pairs constitute pairs of electrons with opposite momentum and spin, formed due to their mutual attraction. In superconductors, these paired electrons move without resistance. The mathematical representation of the Cooper pair wave function is  $\Psi(r_1, \sigma_1, r_2, \sigma_2) = \Phi(r_1 - r_2) \cdot (X_{\uparrow\downarrow} - X_{\downarrow\uparrow})$ , where  $\Psi$  represents the Cooper pair wave function,  $r_1$  and  $r_2$  are the spatial coordinates of the two fermions in the pair,  $\sigma_1$  and  $\sigma_2$  are the spin states of the two fermions,  $\Phi(r_1 - r_2)$  represents the spatial part of the wave function, describing the relative motion of the two fermions,  $X_{\uparrow\downarrow}$  and  $X_{\downarrow\uparrow}$  represent the spin part of the wave function, indicating that the two fermions have opposite spins.



The properties arising from Cooper pairing, such as superfluidity and fermionic nature, make fermions essential resources in the cooling process of quantum computers and superconductors. Superfluidity allows fluids to flow without viscosity or resistance, even at extremely low temperatures. It facilitates reduced decoherence and quantum noise by minimizing thermal energy production. Superfluids also excel as coolants, efficiently absorbing and dissipating heat with minimal resistance, rendering them suitable for cryogenic applications [51].

Cryogenic cooling stands as a primary method for maintaining the exceedingly low temperatures required for the operation of quantum computers. Cryogenic coolers represent specialized refrigeration systems meticulously engineered to reach and sustain temperatures nearing or even touching absolute zero (0 Kelvin or  $-273.15^{\circ}\text{C}$ ), a critical threshold for achieving superconductivity. The cornerstone of these cryogenic coolers is the "Compression-Expansion cycle for cooling." Within this cycle,

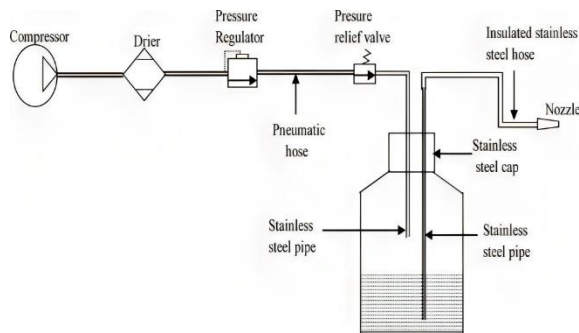


Figure 17: Illustration of a cryogenic cooling system [78]

a working gas, in this context,  $\text{He}^3$ , undergoes a series of compressions and expansions, resulting in a cooling effect for various systems, most notably superconducting quantum computers.

The compression phase commences with the working gas initially at a low pressure and temperature. using compressors and pumps, the gas undergoes a transformation where its pressure and temperature are significantly elevated. Compressors actively exert work on the gas, systematically increasing its pressure, a change that affects its temperature. This relationship adheres to the fundamental ideal gas law:  $PV = nRT$ , where  $P$  represents the gas pressure,  $T$  is its temperature, and  $n$ , the number of moles of gas, remains constant throughout the process.

Employing specialized expansion valves or orifices, the adiabatic expansion phase, signifying a thermodynamic process devoid of heat transfer, executes a rapid expansion of the gas. This adiabatic expansion causes a significant reduction in temperature. The now-cooled gas then causes a reduction in the temperature of the quantum computer, ultimately attaining superconductivity [52].

## V. Superconductors

The superconducting quantum computer stands as a pinnacle in the realm of quantum computing, distinguished by its unparalleled precision in

calculations. This extraordinary computational power hinges on the exploitation of quantum properties inherent to superconductive materials, particularly their manifestation of zero electrical resistance ( $0\ \Omega$ ) and perfect diamagnetism ( $\mu_0$ ).

Zero electrical resistance stems from the formation of Cooper pairs—a phenomenon described earlier. Unlike conventional conductors where electrons traverse the lattice structure of the material, colliding with lattice ions and inducing resistance and heat, superconductors exhibit a distinct behavior [53].

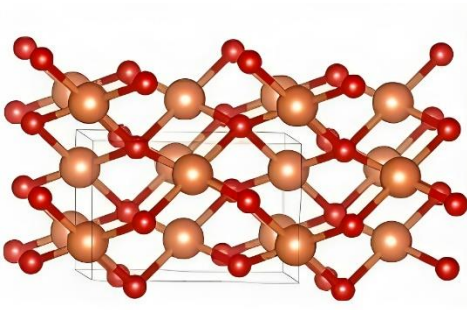


*Figure 18: Lattice structure of copper pairs*

Cooper pairs glide through the lattice without scattering or collisions, behaving as a single entity due to their unique quantum properties and wave function overlap. This unimpeded flow negates the generation of heat and resistance, thus preserving the quantum states of qubits and reducing decoherence.

Perfect diamagnetism is another remarkable property of superconductors, rooted in the Meissner effect. When a superconductor is cooled below its critical temperature ( $T_c$ ) and subjected to an external magnetic field ( $H$ ), it

generates an opposing magnetic field ( $B$ ) within itself. This counteractive field nullifies the external magnetic influence, effectively expelling the magnetic field from the superconductor's interior. The Meissner effect is expressed by the equation  $B = -\mu_0 M$ , wherein  $B$  represents the internal magnetic field,  $\mu_0$  signifies the permeability of free space, and  $M$  denotes the magnetization of the superconductor—a manifestation of the opposing magnetic field. Consequently, the sum of these fields results in a net magnetic flux of zero within the material, resulting in perfect diamagnetism. The total magnetic flux is represented by the equation:  $\Phi = \int \mathbf{B} \cdot d\mathbf{A} = 0$ , where  $\Phi$  is the magnetic flux,  $B$  is the magnetic field, and  $dA$  represents the area over which the integration is performed.

This complete negation of magnetic fields results in the material not being influenced by external forces, reducing decoherence [54].

Coherence in the context of superconducting qubits is a pivotal property denoting the qubit's capacity to exist in a superposition of states while preserving its quantum attributes over an extended duration. It quantifies the qubit's ability to maintain phase and quantum information fidelity. On the contrary, decoherence signifies the undesirable loss of coherence within a quantum system. In the realm of superconducting qubits, decoherence often results from

interactions with the surrounding environment, encompassing factors like thermal fluctuations and electromagnetic noise. This phenomenon imposes temporal limitations on a qubit's ability to uphold its quantum characteristics, thereby impacting the reliability of quantum computations [55, 56].

To address the challenge of decoherence in superconducting qubits, diverse techniques and strategies are employed. Foremost among these is error correction, a multifaceted approach to mitigate errors arising from decoherence and other sources. Quantum error correction codes, such as the surface code, serve as pivotal tools for encoding quantum information redundantly. This redundancy allows for the detection and subsequent correction of errors. Typically, error correction entails the encoding of logical qubits into a greater number of physical qubits, implementation of error-detecting codes and error-correcting procedures, and periodic error monitoring and correction. This intricate process safeguards quantum information from the detrimental consequences of decoherence, enhancing the dependability of quantum computations [57].

Superconductors play a pivotal role in mitigating decoherence due to their exceptional properties. At ultra-low temperatures, these materials manifest zero electrical resistance, enabling the conduction of electricity without energy loss.

This unique trait stems from the formation of Cooper pairs of electrons, which move coherently and devoid of scattering within a material. Furthermore, superconductors exhibit the Meissner effect, expelling magnetic fields entirely from their interior. These characteristics render superconductors invaluable in emerging technologies, particularly quantum computing, where they are instrumental in the creation of qubits with prolonged coherence times [58].

Yttrium Barium Copper Oxide (YBCO) serves as a prominent example of a high-temperature superconductor (HTS) that attains superconducting properties at relatively high temperatures, approximately  $-180^{\circ}\text{C}$  (93.15 K).

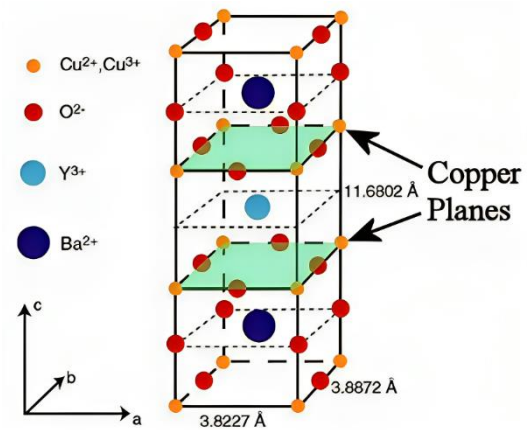


Figure 19: Lattice structure of the Yttrium Barium Copper Oxide HTS

This superconductor finds applications in various domains, encompassing superconducting wires, magnets, and select superconducting qubit implementations [59, 60].

Another notable HTS is Bismuth Strontium Calcium Copper Oxide (BSCCO), which displays superconducting behavior at temperatures over  $-196^{\circ}\text{C}$  (77.15 K). BSCCO materials have a broad range of applications, including utilization in wires, cables, and scientific research, attesting to their versatility [61].

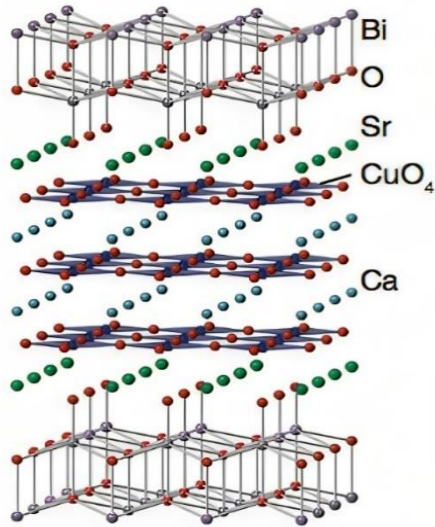


Figure 20: Lattice structure of the Bismuth Strontium Calcium Copper Oxide (BSCCO) HTS

Mercury Barium Calcium Copper Oxide ( $\text{HgBa}_2\text{Ca}_2\text{Cu}_3\text{O}_{8+\delta}$ ) represents yet another example of a high-temperature superconductor. It becomes superconducting at temperatures surpassing  $-150^{\circ}\text{C}$  (123.15 K) and is distinguished for its robust coupling of superconductivity with magnetic properties. This distinctive attribute renders  $\text{HgBa}_2\text{Ca}_2\text{Cu}_3\text{O}_{8+\delta}$  of significant interest both in fundamental research and prospective applications [62].

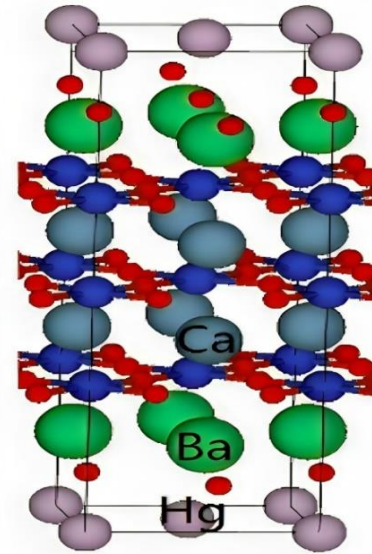


Figure 21: Lattice structure of the Mercury Barium Calcium Copper Oxide HTS [79]

The quest for achieving room-temperature superconductivity stands as a monumental aspiration within the realm of quantum computing. If realized, this breakthrough holds immense potential to revolutionize numerous technological processes. Recent strides have brought this aspiration within closer reach through the introduction of the superconductor known as "LK-99."

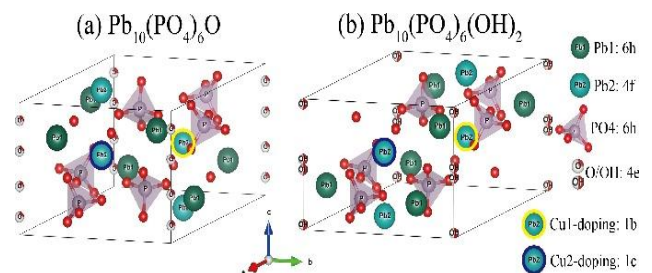


Figure 22: Lattice structure of the LK-99 HTS [80]

Comprising a composition of  $\text{CuPb}_9(\text{PO}_4)_6\text{O}$  and possessing an apatite-like structure, LK-99 has generated considerable attention due to its purported ability to exhibit superconductivity at

temperatures exceeding 400K without necessitating external pressure. This development holds promise for substantially enhancing cost efficiencies in quantum computing and reshaping the quantum computational landscape.

## VI. LK-99

The rise of room-temperature superconductors holds immense promise across a spectrum of industries and scientific endeavors. These materials stand poised to usher in a new era of energy efficiency, particularly in the domain of electrical transmission and distribution, where they have the potential to drastically reduce energy losses within power systems. The implications concerning room-temperature superconductors extend to the realm of electronics, paving the way for more compact and efficient devices, spanning applications from consumer electronics to aerospace. In healthcare, these advanced superconductors could catalyze a revolution in medical technology, particularly in optimizing magnetic resonance imaging (MRI) devices, ultimately enhancing the accessibility and cost-effectiveness of healthcare services. Furthermore, the transportation sector stands to benefit significantly, with the promise of faster, more energy-efficient trains and vehicles, potentially leading to a reduced environmental footprint and improved mobility.

In the field of quantum computing, the advent of room-temperature superconductors carries profound implications. These materials have the potential to significantly enhance qubit stability, a pivotal factor in the efficacy of quantum computers. Among the many qubit technologies, superconducting qubits have shown great promise, and room-temperature superconductors can provide the stable environment necessary for qubits to maintain their quantum states over extended periods. Moreover, the elimination of conventional cryogenic cooling systems, made possible by room-temperature superconductivity, holds the promise of reducing operational costs and complexities associated with quantum computing. This simplified cooling requirement may also streamline the design and scalability of quantum computing systems, potentially enabling the development of large-scale quantum processors with the ability to solve complex problems. Room-temperature superconductors have the potential to democratize quantum computing by alleviating infrastructure and operational barriers, thereby broadening access to this transformative technology across diverse research fields and industries [63-66].

The unique structural characteristics of LK-99, induced by *Cu* doping at *Pb* sites, play a pivotal role in conferring its superconducting properties. This stands in contrast to conventional stress-relieving mechanisms observed in *CuO* and *Fe*-based systems. The mechanism of strain

induction, whether from external forces or internal modifications, underscores the broader concept of strain-induced superconductivity. In the case of LK-99, the subtle contraction of the unit cell volume resulting from  $Cu^{2+}$  substitution for  $Pb^{2+}$  serves as an internal pressure proxy, hypothetically initiating superconductivity within Lead Apatite.

The synthesis of Lanarkite ( $Pb_2SO_5$ ) involves a reaction between  $PbSO_4$  and  $PbO$ , yielding a white powder upon drying. The phase purity is verified through Powder X-ray Diffraction (PXRD). On the other hand, the synthesis of  $Pb_2SO_5$  entails a high-temperature heat treatment at 725°C for 24 hours after mixing  $PbSO_4$  and  $PbO$ .  $Cu_3P$ , another essential component is synthesized via a reaction between  $Cu$  and  $P$  at 550°C for 48 hours. Combining  $Pb_2SO_5$  and  $Cu_3P$  powders in a 1:1 stoichiometric ratio and subjecting them to a final heat treatment at 925°C for 10 hours results in the formation of  $CuPb_9(PO_4)_6O$ , known as LK-99. XRD analysis aligns the polycrystalline samples with JCPDS data. Comprehensive assessments encompass phase purity validation, magnetic levitation experiments, and isothermal magnetization (MH) conducted at 280K on an MPMS SQUID magnetometer, elucidating the magnetic properties of LK-99. This breakthrough beckons for further investigation, particularly regarding its implications for the maintenance

and operational dynamics of quantum computing.

The search mission for room-temperature superconductivity has led to the exploration of several key mechanisms and strategies. Early breakthroughs involved the use of hydrogen sulfide ( $H_2S$ ) under extreme pressures exceeding 100 gigapascals (GPa), which showed traces of superconductivity at relatively high temperatures around 203 K (-70°C). While the high-pressure requirement presents limitations, it underscores the possibility of specific materials exhibiting superconducting behavior under extreme conditions. Hydrogen-saturated compounds, containing hydrogen and other light elements like carbon, have also been the focus of investigation as potential candidates for high-temperature superconductivity due to their high hydrogen content and complex crystal structures. The theoretical prospect of metallic hydrogen, a state where hydrogen transforms into a metal, potentially exhibiting superconductivity at very high temperatures, including room temperature, remains a significant challenge in terms of achievement and stabilization under laboratory conditions. Moreover, researchers are exploring derivatives of hydrogen sulfide that could exhibit superconductivity at more manageable pressures and potentially even higher temperatures. Other avenues of research include mechanical strain engineering, complex computational techniques, utilization of organic materials like molecular

crystals, exploration of multilayered structures, and systematic investigations into pressure-temperature phase diagrams [67-69].

### ***Cryogenic Superconductors***

Cryogenic superconductors, exemplified by materials such as yttrium barium copper oxide (YBCO), demand substantial ongoing maintenance expenditures. For instance, an average-sized facility utilizing cryogenic superconductors incurs annual costs of about \$1 million for cryogenic cooling infrastructure and maintenance. Additionally, the energy consumption for cryogenic systems can be substantial, exceeding \$200,000 annually. Moreover, regular maintenance requirements result in an estimated 5% downtime annually, impacting system reliability and productivity.

### ***LK-99 (Room-Temperature Superconductor)***

In contrast, LK-99, as a room-temperature superconductor, offers the advantage of eliminating cryogenic costs entirely. This translates to potential annual savings of approximately \$1.2 million, encompassing cooling costs, infrastructure maintenance, and energy consumption. Furthermore, the simplified maintenance focus of LK-99, primarily on the superconducting material itself and its integration into the system, leads to a reduction

in annual maintenance costs to approximately \$50,000.

### ***Prospective Financial Advantages of Adopting LK-99***

The adoption of LK-99 carries significant prospective financial advantages. By opting for LK-99 over traditional cryogenic superconductors, organizations can achieve estimated annual savings of around \$1.15 million. This substantial cost reduction is primarily attributed to the elimination of cryogenic infrastructure and associated maintenance costs.

Additionally, LK-99's inherent energy efficiency results in annual savings of approximately \$200,000, making it a cost-effective choice for industries reliant on superconducting technologies. Improved energy efficiency not only reduces operational expenses but also aligns with sustainability goals.

Another crucial aspect is the enhanced reliability of LK-99 systems, with annual downtime reduced to a mere 1%. This improvement in uptime has a direct impact on system reliability and productivity, reducing disruptions and associated costs.

Moreover, industries adopting LK-99, particularly in emerging fields like quantum computing, may gain a competitive edge by simplifying operations and reducing costs. This



could potentially enable them to capture a larger share of the market, further enhancing the financial advantages of LK-99 adoption.

## VII. Conclusion

Examining this research paper has unveiled the influence of LK-99 on the maintenance and operational expenditures associated with quantum computing. It tackles a pivotal challenge that impedes the utilization of quantum computers, namely, the substantial expenses linked to the cooling procedure. This issue could be entirely mitigated by harnessing the room-temperature superconducting capabilities of LK-99, reducing quantum computing's operational costs by \$1.15 million, and enhancing the overall efficiency of the quantum computing process.

## VIII. References

- [1] E. Rieffel and W. Polak, Quantum Computing: A Gentle Introduction. The MIT Press, 2014.
- [2] M. S. Zubairy, “Quantum superposition and entanglement,” Quantum Mechanics for Beginners, pp. 154–171, 2020.  
doi:10.1093/oso/9780198854227.003.0010
- [3] A. Barenco, D. Deutsch, A. Ekert, and R. Jozsa, “Conditional Quantum Dynamics and Logic Gates,” Physical Review Letters, vol. 74, no. 20, pp. 4083–4086, 1995.
- [4] L. K. Grover, “A fast quantum mechanical algorithm for database search,” Proceedings of the twenty-eighth annual ACM symposium on Theory of computing, 1996.  
doi:10.1145/237814.237866
- [5] C. H. Bennett et al., “Teleporting an unknown quantum state via dual classical and Einstein-Podolsky-Rosen channels,” Physical Review Letters, vol. 70, no. 13, pp. 1895–1899, 1993.  
doi:10.1103/physrevlett.70.1895
- [6] C. H. Bennett et al., “Purification of noisy entanglement and faithful teleportation via noisy channels,” Physical Review Letters, vol. 76, no. 5, pp. 722–725, 1996.  
doi:10.1103/physrevlett.76.722
- [7] A. Aspect, J. Dalibard, and G. Roger, “Experimental test of Bell’s inequalities using time-varying analyzers,” Physical Review Letters, vol. 49, no. 25, pp. 1804–1807, 1982.  
doi:10.1103/physrevlett.49.1804
- [8] P. W. Shor, “Scheme for reducing decoherence in Quantum Computer Memory,” Physical Review A, vol. 52, no. 4, 1995. doi:10.1103/physreva.52.r2493

- [9] R. P. Feynman, "Simulating physics with computers," *International Journal of Theoretical Physics*, vol. 21, no. 6–7, pp. 467–488, 1982. doi:10.1007/bf02650179
- [10] W. H. Zurek, "Decoherence, Einselection, and the quantum origins of the classical," *Reviews of Modern Physics*, vol. 75, no. 3, pp. 715–775, 2003. doi:10.1103/revmodphys.75.715
- [11] Michielsen, K., Nocon, M., Willsch, D., Jin, F., Lippert, T., & De Raedt, H. (2017). Benchmarking gate-based quantum computers. *Computer Physics Communications*, 220, 44–55. <https://doi.org/10.1016/j.cpc.2017.06.011>
- [12] Kwon, S., Tomonaga, A., Lakshmi Bhai, G., Devitt, S. J., & Tsai, J.-S. (2021). Gate-based superconducting quantum computing. *Journal of Applied Physics*, 129(4). <https://doi.org/10.1063/5.0029735>
- [13] Fedorov, A., Steffen, L., Baur, M., da Silva, M. P., & Wallraff, A. (2011). Implementation of a Toffoli gate with superconducting circuits. *Nature*, 481(7380), 170–172. <https://doi.org/10.1038/nature10713>
- [14] Barenco, A., Bennett, C. H., Cleve, R., DiVincenzo, D. P., Margolus, N., Shor, P., Sleator, T., Smolin, J. A., & Weinfurter, H. (1995). Elementary Gates for quantum computation. *Physical Review A*, 52(5), 3457–3467. <https://doi.org/10.1103/physreva.52.3457>
- [15] Banchi, L., Pancotti, N., & Bose, S. (2016). Quantum Gate learning in qubit networks: Toffoli Gate without time-dependent control. *Npj Quantum Information*, 2(1). <https://doi.org/10.1038/npjqi.2016.19>
- [16] Yu, N., Duan, R., & Ying, M. (2013). Five two-qubit gates are necessary for implementing the toffoli Gate. *Physical Review A*, 88(1). <https://doi.org/10.1103/physreva.88.010304>
- [17] Roffe, J. (2019). Quantum Error Correction: An introductory guide. *Contemporary Physics*, 60(3), 226–245. <https://doi.org/10.1080/00107514.2019.1667078>
- [18] Devitt, S. J., Munro, W. J., & Nemoto, K. (2013). Quantum error correction for beginners. *Reports on Progress in Physics*, 76(7), 076001. <https://doi.org/10.1088/0034-4885/76/7/076001>

- [19] Cory, D. G., Price, M. D., Maas, W., Knill, E., Laflamme, R., Zurek, W. H., Havel, T. F., & Somaroo, S. S. (1998). Experimental quantum error correction. *Physical Review Letters*, 81(10), 2152–2155.  
<https://doi.org/10.1103/physrevlett.81.2152>
- [20] Liang, L., & Li, C. (2005). Realization of quantum swap gate between flying and stationary qubits. *Physical Review A*, 72(2).  
<https://doi.org/10.1103/physreva.72.024303>
- [21] Tanamoto, T., Liu, Y., Hu, X., & Nori, F. (2009). Efficient quantum circuits for one-way quantum computing. *Physical Review Letters*, 102(10).  
<https://doi.org/10.1103/physrevlett.102.100501>
- [22] Xiang, Z.-L., Ashhab, S., You, J. Q., & Nori, F. (2013). Hybrid quantum circuits: Superconducting circuits interacting with other quantum systems. *Reviews of Modern Physics*, 85(2), 623–653.  
<https://doi.org/10.1103/revmodphys.85.623>
- [23] Möttönen, M., Vartiainen, J. J., Bergholm, V., & Salomaa, M. M. (2004). Quantum circuits for general Multiqubit Gates. *Physical Review Letters*, 93(13).  
<https://doi.org/10.1103/physrevlett.93.130502>
- [24] Zhou, S. S., Loke, T., Izaac, J. A., & Wang, J. B. (2017). Quantum Fourier transform in computational basis. *Quantum Information Processing*, 16(3).  
<https://doi.org/10.1007/s11128-017-1515-0>
- [25] Jozsa, R. (1998). Quantum algorithms and the Fourier transform. *Proceedings of the Royal Society of London. Series A: Mathematical, Physical and Engineering Sciences*, 454(1969), 323–337.  
<https://doi.org/10.1098/rspa.1998.0163>
- [26] O’Brien, T. E., Tarasinski, B., & Terhal, B. M. (2019). Quantum phase estimation of multiple eigenvalues for small-scale (noisy) experiments. *New Journal of Physics*, 21(2), 023022.  
<https://doi.org/10.1088/1367-2630/aafb8e>
- [27] Chapeau-Blondeau, F., & Belin, E. (2020). Fourier-transform quantum phase estimation with Quantum Phase Noise. *Signal Processing*, 170, 107441.  
<https://doi.org/10.1016/j.sigpro.2019.107441>
- [28] Dorner, U., Demkowicz-Dobrzanski, R., Smith, B. J., Lundeen, J. S., Wasilewski, W., Banaszek, K., & Walmsley, I. A. (2009). Optimal Quantum Phase Estimation.

Physical Review Letters, 102(4).  
<https://doi.org/10.1103/physrevlett.102.040403>

- [29] J. Choi and J. Kim, "A Tutorial on Quantum Approximate Optimization Algorithm (QAOA): Fundamentals and Applications," 2019 International Conference on Information and Communication Technology Convergence (ICTC), Jeju, Korea (South), 2019, pp. 138-142, doi: 10.1109/ICTC46691.2019.8939749.

- [30] Zhou, L., Wang, S.-T., Choi, S., Pichler, H., & Lukin, M. D. (2020). Quantum approximate optimization algorithm: Performance, mechanism, and implementation on near-term devices. *Physical Review X*, 10(2).  
<https://doi.org/10.1103/physrevx.10.021067>

- [31] C. C. McGeoch, R. Harris, S. P. Reinhardt and P. I. Bunyk, "Practical Annealing-Based Quantum Computing," in *Computer*, vol. 52, no. 6, pp. 38-46, June 2019, doi: 10.1109/MC.2019.2908836.

- [32] Dziarmaga, J. (2005). Dynamics of a quantum phase transition: Exact solution of the Quantum Ising model. *Physical Review Letters*, 95(24).

[<https://doi.org/10.1103/physrevlett.95.245701>](<https://doi.org/10.1103/physrevlett.95.245701>)

- [33] Chakravarty, S. (1982). Quantum fluctuations in the tunneling between superconductors. *Physical Review Letters*, 49(9), 681–684.  
<https://doi.org/10.1103/physrevlett.49.681>
- [34] Bruinsma, R., & Bak, P. (1986). Quantum tunneling, dissipation, and fluctuations. *Physical Review Letters*, 56(5), 420–423.  
<https://doi.org/10.1103/physrevlett.56.420>
- [35] J. Clarke and F. K. Wilhelm, "Superconducting Quantum Bits," *Nature*, vol. 453, no. 7198, pp. 1031–1042, 2008.  
doi:10.1038/nature07128
- [36] R. Barends et al., "Superconducting quantum circuits at the surface code threshold for fault tolerance," *Nature*, vol. 508, no. 7497, pp. 500–503, 2014.  
doi:10.1038/nature13171
- [37] M. Tinkham and V. Emery, "introduction to superconductivity," *Physics Today*, vol. 49, no. 10, pp. 74–74, 1996.  
doi:10.1063/1.2807811
- [38] J. E. Mooij et al., "Josephson persistent-current qubit," *Science*, vol. 285, no. 5430, pp. 1036–1039, 1999.

doi:10.1126/science.285.5430.103

Nature, vol. 445, no. 7127, pp. 515–518, 2007. doi:10.1038/nature05461

- [39] G. Wendin and V. S. Shumeiko, “Quantum Bits with Josephson Junctions (review article),” *Low Temperature Physics*, vol. 33, no. 9, pp. 724–744, 2007. doi:10.1063/1.2780165
- [40] J. Koch et al., “Charge-insensitive qubit design derived from the Cooper Pair Box,” *Physical Review A*, vol. 76, no. 4, 2007. doi:10.1103/physreva.76.042319
- [41] P. Krantz et al., “A Quantum Engineer’s Guide to superconducting qubits,” *Applied Physics Reviews*, vol. 6, no. 2, 2019. doi:10.1063/1.5089550
- [42] E. T. Jaynes and F. W. Cummings, “Comparison of quantum and semiclassical radiation theories with application to the beam maser,” *Proceedings of the IEEE*, vol. 51, no. 1, pp. 89–109, 1963. doi:10.1109/proc.1963.1664
- [43] A. Wallraff et al., “Strong coupling of a single photon to a superconducting qubit using circuit quantum electrodynamics,” *Nature*, vol. 431, no. 7005, pp. 162–167, 2004. doi:10.1038/nature02851
- [44] D. I. Schuster et al., “Resolving photon number states in a superconducting circuit,” *Nature*, vol. 445, no. 7127, pp. 515–518, 2007. doi:10.1038/nature05461
- [45] Feng, J.-J., Wu, B., & Wilczek, F. (2022). Quantum computing by Coherent Cooling. *Physical Review A*, 105(5). <https://doi.org/10.1103/physreva.105.052601>
- [46] Kwon, D., Bae, J., & Jeong, S. (2022). Development of the integrated sorption cooler for an adiabatic demagnetization refrigerator (ADR). *Cryogenics*, 122, 103421. <https://doi.org/10.1016/j.cryogenics.2022.103421>
- [47] Radebaugh, R. (1990). A Review of Pulse Tube Refrigeration. In: Fast, R.W. (eds) *Advances in Cryogenic Engineering*. *Advances in Cryogenic Engineering*, vol 35. Springer, Boston, MA. [https://doi.org/10.1007/978-1-4613-0639-9\\_143](https://doi.org/10.1007/978-1-4613-0639-9_143)
- [48] de Waele, A. T. A. M. (2000). Pulse-tube refrigerators: Principle, recent developments, and prospects. *Physica B: Condensed Matter*, 280(1–4), 479–482. [https://doi.org/10.1016/s0921-4526\(99\)01840-2](https://doi.org/10.1016/s0921-4526(99)01840-2)

- [49] Radebaugh, R., Zimmerman, J., Smith, D.R., Louie, B. (1986). A Comparison of Three Types of Pulse Tube Refrigerators: New Methods for Reaching 60K. In: Fast, R.W. (eds) *Advances in Cryogenic Engineering*. Advances in Cryogenic Engineering, vol 31. Springer, Boston, MA. [https://doi.org/10.1007/978-1-4613-2213-9\\_88](https://doi.org/10.1007/978-1-4613-2213-9_88)
- [50] Fujita, S., & Godoy, S. (2002). Liquid Helium: Bose–Einstein Condensation. In *Quantum Statistical Theory of Superconductivity* (1st ed., Vol. 338, pp. 67–74). essay, Kluwer Academic Publishers.
- [51] Kaplan, I. G. (2017). Construction of Functions with a Definite Permutation Symmetry. In *The Pauli Exclusion Principle: Origin, verifications and applications* (1st ed., Vol. 228, pp. 25–49). essay, Wiley.
- [52] Ross, R. G. (2016). Chapter 6 refrigeration systems for achieving cryogenic temperatures. *Low Temperature Materials and Mechanisms*, 109–182. <https://doi.org/10.1201/9781315371962-7>
- [53] Huang, H.-L., Wu, D., Fan, D., & Zhu, X. (2020). Superconducting quantum computing: A Review. *Science China Information Sciences*, 63(8).
- [54] Bouchiat, V., Vion, D., Joyez, P., Esteve, D., & Devoret, M. H. (1998). Quantum coherence with a single Cooper pair. *Physica Scripta*, T76(1), 165. <https://doi.org/10.1238/physica.topical.076a00165>
- [55] Duan, L.-M., & Guo, G.-C. (1997). Preserving coherence in quantum computation by pairing quantum bits. *Physical Review Letters*, 79(10), 1953–1956. <https://doi.org/10.1103/physrevlett.79.1953>
- [56] Unruh, W. G. (1995). Maintaining coherence in quantum computers. *Physical Review A*, 51(2), 992–997. <https://doi.org/10.1103/physreva.51.992>
- [57] Duan, L.-M., & Guo, G.-C. (1998). Reducing decoherence in quantum-computer memory with all quantum bits coupling to the same environment. *Physical Review A*, 57(2), 737–741. <https://doi.org/10.1103/physreva.57.737>
- [58] K. Ilieva and O. Dinolov, "State-of-the-art of superconducting materials and their energy-efficiency applications," 2020 7th International Conference on Energy

Efficiency and Agricultural Engineering (EE&AE), Ruse, Bulgaria, 2020, pp. 1-5, doi:10.1109/EEAE49144.2020.9279004.

- [59] Hannachi, E., Sayyed, M. I., Almuqrin, A. H., & Mahmoud, K. G. (2021). Study of the structure and radiation-protective properties of yttrium barium copper oxide ceramic doped with different oxides. *Journal of Alloys and Compounds*, 885, 161142. <https://doi.org/10.1016/j.jallcom.2021.161142>
- [60] Ionescu, M., Ramer, R., Constantin, C., Ribco, L., Russell, G., Ramer, A., & Fagan, J. (1996). Properties of yttrium barium copper oxide (YBCO) containing vanadium. *Electric Power Systems Research*, 36(3), 139–143. [https://doi.org/10.1016/0378-7796\(95\)00963-9](https://doi.org/10.1016/0378-7796(95)00963-9)
- [61] Berry, A. D., Holm, R. T., Cukauskas, E. J., Fatemi, M., Gaskill, D. K., Kaplan, R., & Fox, W. B. (1988). Growth of superconducting thin films of bismuth-strontium-calcium-copper oxide by organometallic chemical vapor deposition. *Journal of Crystal Growth*, 92(1–2), 344–347. [https://doi.org/10.1016/0022-0248\(88\)90470-8](https://doi.org/10.1016/0022-0248(88)90470-8)
- [62] Babych, O., Boyko, Y., Gabriel, I., Luticiv, R., Matviyiv, M., Sadovy, B., & Vasyuk, M. (2011). Synthesis and properties of doped  $\text{HgBa}_2\text{Ca}_2\text{Cu}_3\text{O}_{8+\delta}$  superconductors. *Journal of Physics: Conference Series*, 289, 012015. <https://doi.org/10.1088/1742-6596/289/1/012015>
- [63] Guo, K., Li, Y. & Jia, S. Ferromagnetic half levitation of LK-99-like synthetic samples. *Sci. China Phys. Mech. Astron.* 66, 107411 (2023). <https://doi.org/10.1007/s11433-023-2201-9>
- [64] Goldoni, R. (2023). LK-99 Perpetual Review: A Collaborative Effort to Curate a Living Document on the Discovery of LK-99. <https://doi.org/10.55277/researchhub.jhtse6tt>
- [65] Zhang, Z. (2023). The event and skepticism for the electrical conductor LK-99 at ambient temperature and pressure. *Superconductivity*, 100059. <https://doi.org/10.1016/j.supcon.2023.100059>
- [66] Garisto, D. (2023). Claimed superconductor LK-99 is an online sensation — but replication efforts fall short. *Nature*, 620



(7973), 253–253.

<https://doi.org/10.1038/d41586-023-02481-0>.

[67] Kumar, K., Karn, N. K., & Awana, V. P. (2023). Synthesis of possible room temperature superconductor LK-99: Pb9Cu(Po4)6O. *Superconductor Science and Technology*, 36(10).

<https://doi.org/10.1088/1361-6668/acf002>

[68] Biswas, S., & Awal, S. S. (2023). Potential role of room temperature superconductor LK 99 in MRI and radiology, if true. *SSRN Electronic Journal*.

<https://doi.org/10.2139/ssrn.4533054>.

[69] Lai, J., Li, J., Liu, P., Sun, Y., & Chen, X.-Q. (2024). First-principles study on the electronic structure of PB10–CU (PO4)6O (x=0, 1). *Journal of Materials Science & Technology*, 171, 66–70.

<https://doi.org/10.1016/j.jmst.2023.08.001>

[70] Q. Zhao et al., “Fault-tolerant quantum error correction code preparation in UBQC,” *Quantum Information Processing*, vol. 19, no. 8, 2020. doi:10.1007/s11128-020-02735-0

[71] J. P. Hayes and I. L. Markov, *Quantum Approaches to Logic Circuit Synthesis and*

*Testing*. United States, Michagen: Michigan univ ann arbor, 2006

[72] M. Chandran, “Critical state in thin superconductors: A josephson junction array analogy,” *Physica C: Superconductivity*, vol. 292, no. 1–2, pp. 147–157, 1997. doi:10.1016/s0921-4534(97)01633-x

[73] X.-P. Zhang, L.-T. Shen, Z.-Q. Yin, H.-Z. Wu, and Z.-B. Yang, “Resonator-assisted Quantum Bath Engineering of a flux qubit,” *Physical Review A*, vol. 91, no. 1, 2015. doi:10.1103/physreva.91.013825

[74] J. A. Blackburn, M. Cirillo, and N. Grønbech-Jensen, “A survey of classical and quantum interpretations of experiments on Josephson junctions at very low temperatures,” *Physics Reports*, vol. 611, pp. 1–33, 2016. doi:10.1016/j.physrep.2015.10.010

[75] H. He-Liang, “Quantum computing,” *Quantum Information and Quantum Optics with Superconducting Circuits*, pp. 198–238, 2022. doi:10.1017/9781316779460.008

[76] S. Carretta et al., “Quantum Information Processing with hybrid spin-photon qubit encoding,” *Physical Review Letters*, vol.

111, no. 11, 2013.

doi:10.1103/physrevlett.111.110501

- [77] K. Uhlig, “Cryogen-free dilution refrigerator precooled by a pulse-tube refrigerator with non-magnetic regenerator,” AIP Conference Proceedings, 2006. doi:10.1063/1.2202505
- [78] M. Dhananchezian, M. P. Kumar, and T. Sornakumar, “Cryogenic turning of Aisi 304 stainless steel with modified tungsten carbide tool inserts,” Materials and Manufacturing Processes, vol. 26, no. 5, pp. 781–785, 2011.  
doi:10.1080/10426911003720821
- [79] Qiu, Y., Li, H., Liu, Y., Chi, B., Pu, J., & Li, J. (2020). Effects of niobium doping on the stability of  $\text{SrCo}_{0.2}\text{Fe}_{0.8}\text{O}_{3-\delta}$  cathodes for intermediate temperature solid oxide fuel cells. *Journal of Alloys and Compounds*, 829, 154503.  
<https://doi.org/10.1016/j.jallcom.2020.154503>
- [80] T. Liao, T. Sasaki, and Z. Sun, “The oxygen migration in the apatite-type lanthanum silicate with the cation substitution,” *Physical Chemistry Chemical Physics*, vol. 15, no. 40, p. 17553, 2013.  
doi:10.1039/c3cp52245h